

## **Fe<sub>3</sub>O<sub>4</sub>/Carbon quantum dots hybrid nanoflowers for highly active and recyclable visible-light driven photocatalyst**

Hui Wang,<sup>a</sup> Zengyan Wei,<sup>b</sup> Hiroshi Matsui,<sup>b</sup> and Shuiqin Zhou<sup>\*,a</sup>

<sup>a</sup>Department of Chemistry of The College of Staten Island and The Graduate Center, The City University of New York, Staten Island, NY 10314, USA

<sup>b</sup>Department of Chemistry and Biochemistry, Hunter College, The City University of New York, New York, NY 10065

### **Experimental Section**

All chemicals were purchased from Sigma-Aldrich. In a typical synthesis, ferrocene (0.10 g) were dissolved in an acetone (30 mL). After intense sonication for 30 min, 6.0 mL of 30% H<sub>2</sub>O<sub>2</sub> solution was slowly added into the solution, which was then vigorously stirred for 30 min with a magnetic stirring apparatus. The precursor solution was then transferred to a 50.0 mL Teflon-lined stainless autoclave and heated to and maintained at 200 °C. After 48 h reaction, the autoclave was cooled naturally to room temperature and intensively sonicated for 15 min. The products from the Teflon-lined stainless autoclave were then magnetized for 30 min by a magnet with 0.30 T. The supernatant was discarded under a magnetic field. The precipitates were washed with acetone three times to remove possible excess ferrocene. Finally, the black products were dried at room temperature in a vacuum oven.

Photocatalytic degradation of methylene blue (MB) was carried out in a 20 mL vial containing 1 mL MB solution ( $2 \times 10^{-3}$  mol L<sup>-1</sup>), 1 mL of fresh NaOH solution (0.01 mol L<sup>-1</sup>) and a suitable amount (1 mg) of Fe<sub>3</sub>O<sub>4</sub>@CQDs hybrid NFs as the catalyst. The visible light was provided by a Xenon lamp (75 W) with an optical filter cutting off wavelengths below 420 nm. The quantity of MB in the reaction solution was determined spectrophotometrically at  $\lambda_{\text{max}} = 665$  nm. After 1 h reaction, the catalyst was quickly separated and collected

from the solution using a NdFeB magnet, and then rinsed with a large amount of water. The recovered catalyst was dried and then re-dispersed into a mixture of new reactants to initiate second reaction cycle. The same procedure was performed in the additional cycles.

TEM and HRTEM images were obtained by JEM 2100 (JEOL) with an acceleration voltage of 200 kV. Energy-dispersive X-ray (EDX) analysis was obtained with an EDAX detector installed on the same HRTEM. Raman spectrum was taken on a LABRAM-HR Confocal Laser Micro-Raman spectrometer using an Ar<sup>+</sup> laser ( $\lambda = 514.5$  nm) at room temperature. The FT-IR spectrum was recorded with a Nicolet Instrument Co. MAGNA-IR 750 Fourier transform infrared spectrometer. The PL study was carried out on a JOBIN YVON Co. FluoroMax<sup>®</sup>-3 Spectrofluorometer, and UV/Vis spectra were obtained on a Thermo Electron Co. Helios  $\beta$  UV-vis Spectrometer. A superconducting quantum interference device magnetometer (Quantum Design MPMS XL-7) was used to measure the magnetic properties of as-prepared samples.

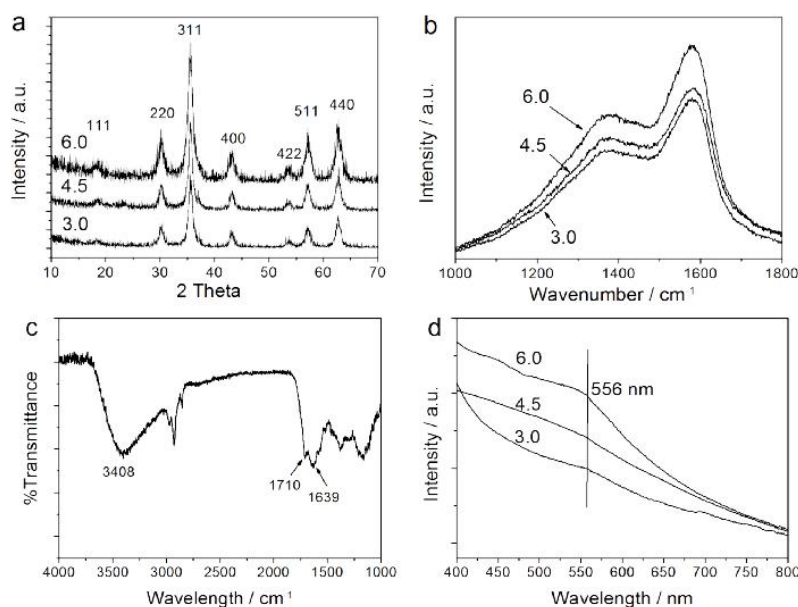


**Figure S1.** (a) XRD patterns, (b) Raman spectra, (c) FT-IR spectrum, and (d) UV-vis spectra in visible light region of the Fe<sub>3</sub>O<sub>4</sub>@CQDs hybrid NFs synthesized with different amount of H<sub>2</sub>O<sub>2</sub> in reaction medium.

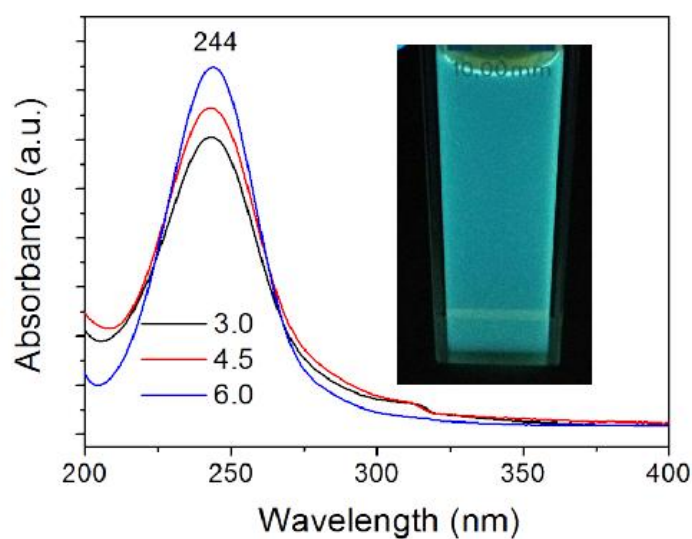


**Figure S2.** UV-vis spectra of the Fe<sub>3</sub>O<sub>4</sub>@CQDs hybrid NFs prepared with different amount of H<sub>2</sub>O<sub>2</sub>. The inset shows the photo of Fe<sub>3</sub>O<sub>4</sub>@CQDs-6.0 NFs dispersed in water under a UV light of 365 nm.

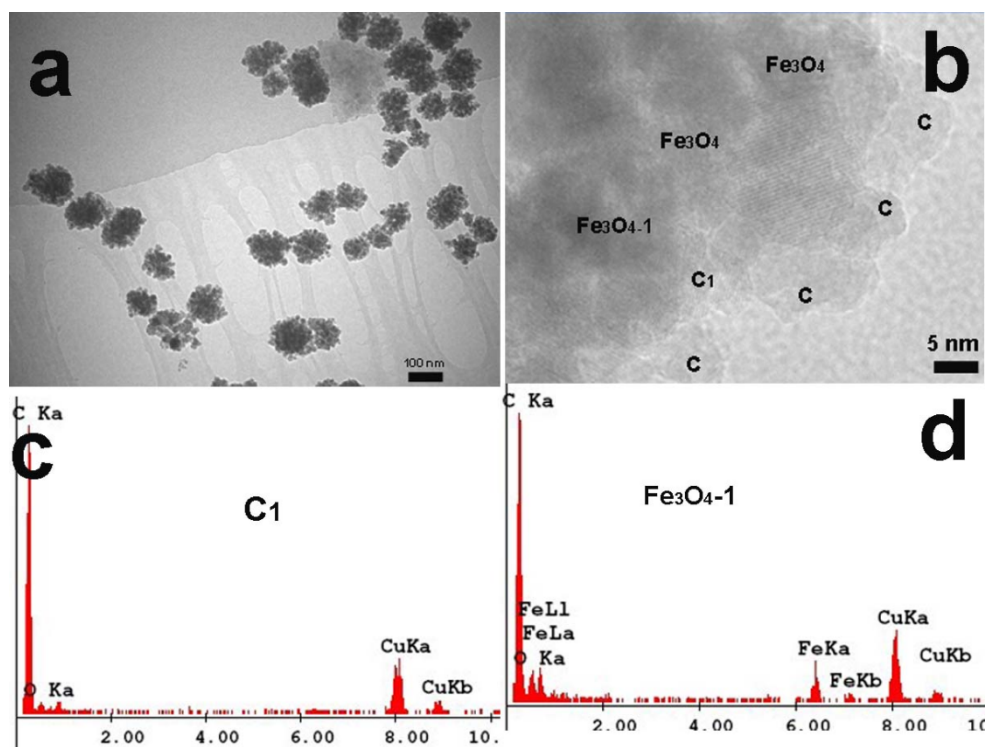


**Figure S3.** (a) TEM image of the Fe<sub>3</sub>O<sub>4</sub>@CQDs-3.0 hybrid NFs; (b) High resolution TEM image of the sectional Fe<sub>3</sub>O<sub>4</sub>@CQDs-3.0 hybrid NF showing single CQDs and Fe<sub>3</sub>O<sub>4</sub> nanocrystals; (c) and (d) Energy dispersive spectrum of the CQDs in shell and nanocrystals in the core, respectively.

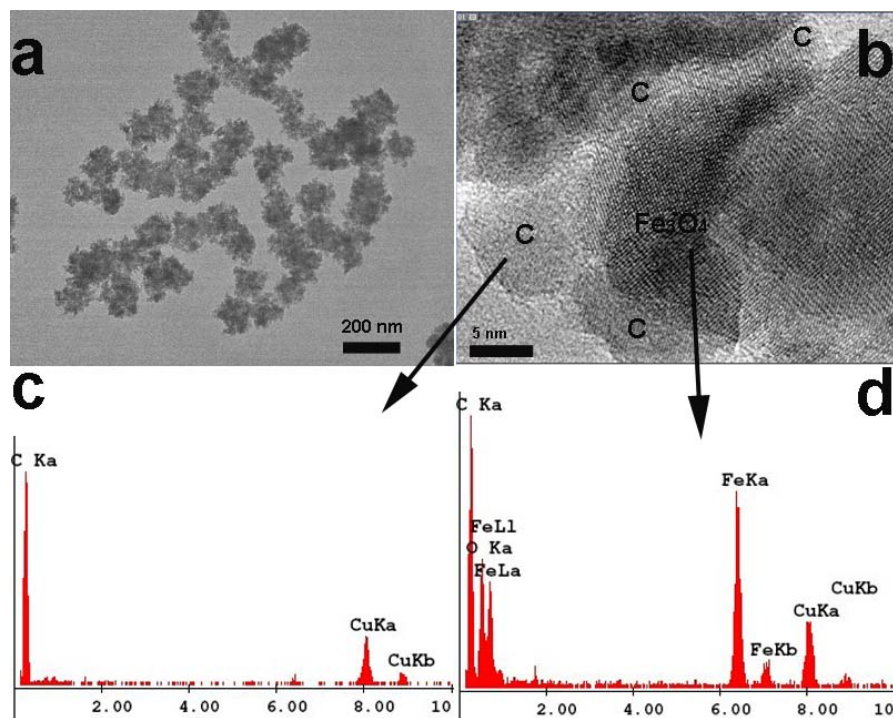


**Figure S4.** (a) TEM image of the  $\text{Fe}_3\text{O}_4@\text{CQDs}$ -4.5 hybrid NFs; (b) High resolution TEM image of the sectional  $\text{Fe}_3\text{O}_4@\text{CQDs}$ -4.5 hybrid NF showing single CQDs and  $\text{Fe}_3\text{O}_4$  nanocrystals; (c) and (d) Energy dispersive spectrum of the CQDs in shell and nanocrystals in the core, respectively.

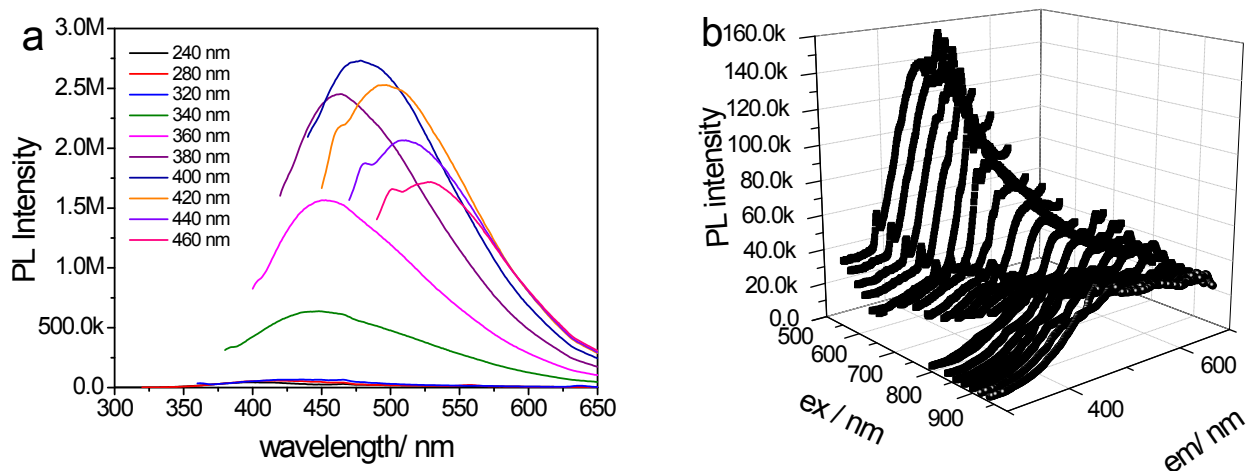


**Figure S5.** (a) PL spectra and (b) upconverted PL spectra of the  $\text{Fe}_3\text{O}_4@\text{CQDs}$ -3.0 hybrid NFs.

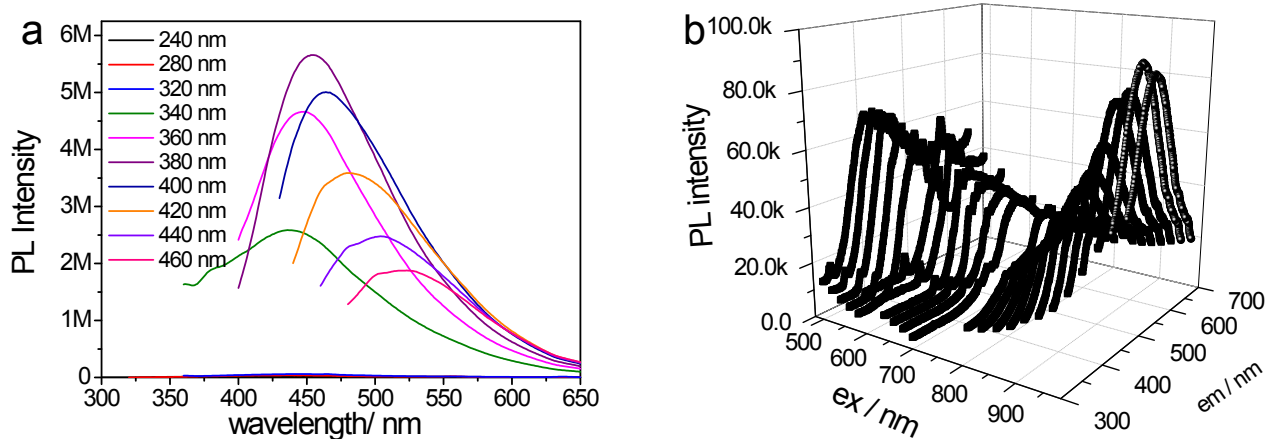


**Figure S6.** (a) PL spectra and (b) upconverted PL spectra of the  $\text{Fe}_3\text{O}_4@\text{CQDs-4.5}$  hybrid NFs.

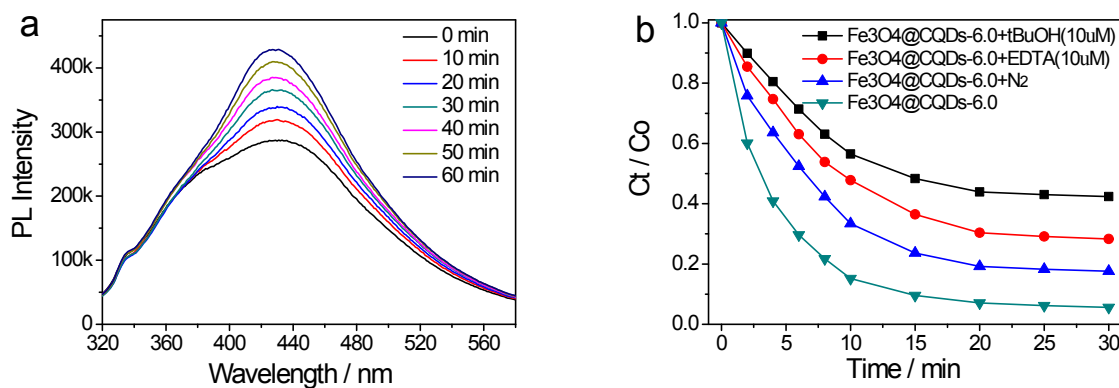


**Figure S7.** a) Time-dependent fluorescence emission spectra of TAOH formed by the reaction of TA with  $\bullet\text{OH}$  radicals generated by the  $\text{Fe}_3\text{O}_4@\text{CQDs-6.0}$  NFs photocatalyst under visible-light irradiation. b) The photodegradation profiles of MB in the presence of the  $\text{Fe}_3\text{O}_4@\text{CQDs-6.0}$  photocatalyst (with different conditions) under visible-light irradiation with cutting off 420 nm.

The  $\bullet\text{OH}$  radicals produced by the  $\text{Fe}_3\text{O}_4@\text{CQDs-6.0}$  NFs photocatalyst under visible-light irradiation could be probed using a method described previously.<sup>S1,S2</sup> It is known that  $\bullet\text{OH}$  reacts with terephthalic acid (TA) in basic solution to generate 2-hydroxyterephthalic acid (TAOH), which emits a unique fluorescence signal with its peak centered at  $\sim 427\text{nm}$ . Figure S7a clearly shows a gradual enhancement of the fluorescence intensity associated with TAOH upon the increase in the irradiation time of  $\text{Fe}_3\text{O}_4@\text{CQDs}$  photocatalyst under visible light. This result supports our mechanism that the photo-excited holes in the  $\text{Fe}_3\text{O}_4@\text{CQDs}$  catalyst are powerful

enough to oxidize surface-adsorbed hydroxyl groups and water to generate  $\cdot\text{OH}$  radicals. Furthermore, we have carried out several experimental measurements for the time dependent photodegradation fraction of MB in the presence of  $\text{N}_2$  purging, hole scavenger EDTA, and a hydroxyl radical scavenger tBuOH, respectively. The  $\text{N}_2$  purging should reduce the amount of  $\text{O}_2$  adsorbed on the surface of catalyst and thus reduce the active oxygen radicals (e.g.,  $\cdot\text{O}_2^-$ ). The hole or hydroxyl radical scavenger will reduce the amount of active hydroxyl radicals. Both can suppress the degradation of MB solution. In fact, as shown in Figure S7b, compared to the control catalytic activity of  $\text{Fe}_3\text{O}_4@\text{CQDs}$ -6.0 NFs (95.8% of MB degraded after 30 min), the photodegradation fraction of MB is decreased to 82.5%, 71.7%, and 57.7% in the presence of  $\text{N}_2$  purging, 1  $\mu\text{M}$  EDTA, and 1  $\mu\text{M}$  tBuOH, respectively. These results further support our proposed catalytic mechanism that the adsorbed  $\text{O}_2$  and  $\text{H}_2\text{O}/\text{OH}^-$  on the surface of the catalyst will react with the separated photo-generated electrons and holes to produce the active free radicals like  $\cdot\text{O}_2^-$  and  $\cdot\text{OH}$ , which in turn effectively degrade the MB.

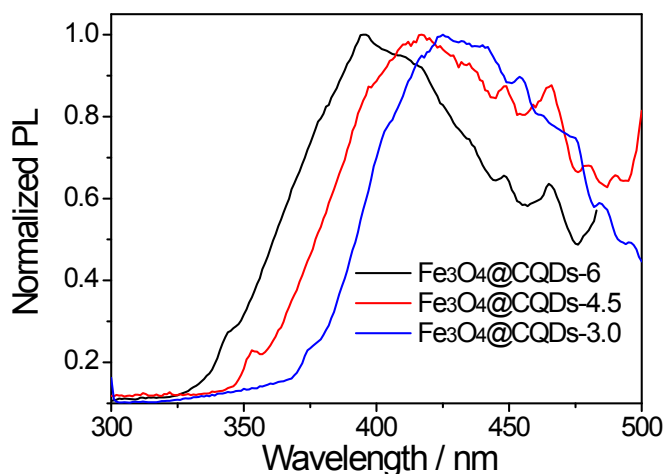


**Figure S8.** Upconverted PL spectra of the  $\text{Fe}_3\text{O}_4@\text{CQDs}$  hybrid NFs synthesized with different amount of  $\text{H}_2\text{O}_2$ , obtained with an excitation wavelength of 556 nm.

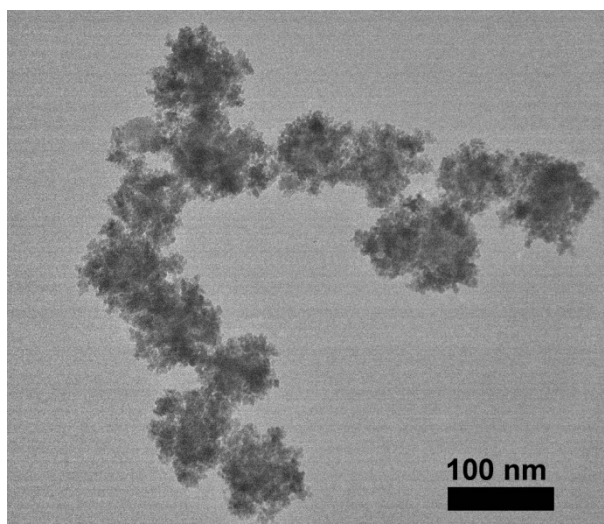


**Figure S9.** TEM image of the recycled Fe<sub>3</sub>O<sub>4</sub>@CQDs-6.0 hybrid NFs after 10 runs of catalytic photodegradation of MB and recycling.

[S1] J. H. Huang, K. N. Ding, X. C. Wang, X. Z. Fu, *Langmuir*, 2009, **25**, 8313.

[S2] G. Liu, P. Niu, L. C. Yin, H. M. Cheng, *J. Am. Chem. Soc.*, 2012, **134**, 9070.